COM-RP-MPE-DRG-171

Studying the ToF Spectrum as a Function of Energy Part 2: the Forward Peak Region

prepared by Georg Weidenspointner (MPE)

and Martin Varendorff (MPE)

November 7, 1996

1 Introduction

The basic problems concerning the ToF (time of flight) distribution outlined in the introduction of the report *Studying the ToF Spectrum as a Function of Energy Part 1: the Forward Peak Region* (`COM-RP-MPE-DRG-165`) by G. Weidenspointner and M. Varendorff are still unresolved. This first analysis was based on $\mathrm{ToF}_{\mathrm{II}}$ data[1]. As was pointed out there, some improvements would be expected if $\mathrm{ToF}_{\mathrm{III}}$ data were used.

The purpose of this report is to redo the analysis summarized in `COM-RP-MPE-DRG-165` using $\mathrm{ToF}_{\mathrm{III}}$ data, as described in Section 2. A quantitative comparison of the results obtained with $\mathrm{ToF}_{\mathrm{II}}$ and $\mathrm{ToF}_{\mathrm{III}}$ data is given in Section 3.

Whenever detailed explanations of certain aspects and problems of the analysis have already been given in `COM-RP-MPE-DRG-165` the description can be rather brief in this report. Therefore reading `COM-RP-MPE-DRG-165` before reading this report is recommended.

[1] $\mathrm{ToF}_{\mathrm{II}}$ data are ToF data that have been corrected with `TOFCOR` written by Rob van Dijk. The corrections applied there are based on the E1 and E2 energy deposits. A better correction can be made based on the D1 and D2 analog sums. This is done in `IFCTCF`, also written by Rob van Dijk, which returns $\mathrm{ToF}_{\mathrm{III}}$ data. For details concerning ToF in general and these ToF corrections in particular, refer to `COM-RP-ROL-DRG-62` by Rob van Dijk or his PhD thesis.

2 Data Base and Fitting Procedure

This analysis is essentially the same as the one in `COM-RP-MPE-DRG-165`. Therefore only differences between the current and the former analysis are briefly summarized in this Section.

2.1 Data Base

The data base of the current analysis consists of `GAMMA-1` data that was run through `IFCTCF` to obtain ToF values of the highest quality ($\mathrm{ToF_{III}}$). The following OPs were used: 204 - 207, 209, 210, 222, 223, 231, 301, 302.3, 304 - 306, 308.6, 312, 313, 317, 320 - 324, 326, 330, 334, 406 - 408, 414.3, 421, 429, 501, 508, 509, 511, 511.5, 513, 514 and 517. In total this data base consists of 43 OPs containing about 1.1×10^7 events in 180793 superpackets. These OPs were selected because they allowed the gathering of data during times when

$$\texttt{GCEL} \geq 140°.$$

The following event selections were applied to accumulate the data base:

$$\begin{gathered} 800 \text{ keV} \leq \text{Etot} \leq 30 \text{ MeV} \\ 70 \text{ keV} \leq \text{E1} \leq 20 \text{ MeV} \\ 730 \text{ keV} \leq \text{E2} \leq 30 \text{ MeV} \\ 100 \text{ channels} \leq \text{ToF} \leq 150 \text{ channels} \\ \text{PSD} \leq 110 \text{ channels} \\ \bar{\varphi} \leq 50° \end{gathered}$$

In addition, the modules D2-01 and D2-02 were excluded, as were some areas in D2-11, D2-13 and D2-14 due to PMT failure according to the `SKYDRI` convention.

In the analysis the following additional event selections were applied:

$$\begin{gathered} 6° \leq \bar{\varphi} \leq 40° \\ \xi \leq 40° \end{gathered}$$

The PSD cut applied in the analysis was energy dependent (based on a comparison of cosmic diffuse background simulations and real data). For 800 keV $\leq$ Etot $\leq$ 4 MeV (with Etot in [MeV]):

$$\mathrm{PSD}_{low}(\mathrm{Etot}) = \frac{\lg \mathrm{Etot} - \lg 0.8}{\lg 4 - \lg 0.8} \cdot (70 - 55) + 55 \quad [\text{channel}]$$

$$\mathrm{PSD}_{up}(\mathrm{Etot}) = 100 - \frac{\lg \mathrm{Etot} - \lg 0.8}{\lg 4 - \lg 0.8} \cdot (100 - 90) \quad [\text{channel}]$$

Thus PSD_{low} varies logarithmically with Etot from 55 channels at 800 keV to 70 channels at 4 MeV and PSD_{up} varies logarithmically with Etot from 100 channels at 800 keV to 90 channels at 4 MeV. Above 4 MeV:

$$\begin{gathered} \mathrm{PSD}_{low}(\mathrm{Etot}) = 70 \\ \mathrm{PSD}_{up}(\mathrm{Etot}) = 90 \end{gathered}$$

These boundaries are determined by the available simulation data (see `COM-RP-ROL-DRG-44` by Rob van Dijk and `COM-RP-MPE-SIM-3` by G. Weidenspointner). The distribution of the real data suggests a smaller range, but this range is not properly accessible by simulation.

2.2 Fitting Procedure

2.2.1 ToF Spectra

See `COM-RP-MPE-DRG-165`: the energy range was divided in 200 bins such that each bin contained about the same number of events. All ToF spectra were corrected for the lifetime of the telescope. The curent analysis also includes data from Phases 4 and 5, when the activation of the spacecraft was high, which changed the overall energy spectrum. Therefore the resulting energy binning for this analysis is different from that used in the former study.

2.2.2 Models

See `COM-RP-MPE-DRG-165`: in the analyses of the ToF distribution as a function of energy the forward peak was always represented by a gaussian. The ToF continuum in the forward peak region was described by three different simple analytical functions: a parabola, a gaussian and an exponential. The three energy dependent models are listed below.

Parabolic Model

$$f_p(tof,E) = p_1(E)\cdot\exp\left(-\frac{1}{2}\left(\frac{tof-p_2(E)}{p_3(E)}\right)^2\right) + p_4(E)\cdot(tof-p_5(E))^2 + p_6(E)$$

Gaussian Model

$$f_g(tof,E) = p_1(E)\cdot\exp\left(-\frac{1}{2}\left(\frac{tof-p_2(E)}{p_3(E)}\right)^2\right) + p_4(E)\cdot\exp\left(-\frac{1}{2}\left(\frac{tof-80}{p_5(E)}\right)^2\right) + p_6(E)$$

Exponential Model

$$f_e(tof,E) = p_1(E)\cdot\exp\left(-\frac{1}{2}\left(\frac{tof-p_2(E)}{p_3(E)}\right)^2\right) + p_4(E)\cdot\exp\left(\frac{97.5}{p_5(E)}\right)\cdot\exp\left(-\frac{tof}{p_5(E)}\right) + p_6(E)$$

In the gaussian model the center of the gaussian describing the continuum background was fixed at ToF=80, the approximate position of the backward peak.

2.2.3 Difficulties

The basic problems are outlined in `COM-RP-MPE-DRG-165`. The general behaviour of the three models didn't change: the parabolic model is the most robust; the exponential model and the gaussian model are more likely to “fail” (as explained in the earlier report).

The parabolic model was first fitted over a “wide” range, ToF=106 to ToF=144, at all energies. As was to be expected, a parabola cannot describe the shape of the ToF continuum over such a wide range. Therefore a set of energy dependent “narrow” fit ranges

Energy Range [MeV]	Fit Range [ToF channel]			
	Parabola wide	Parabola narrow	Exponential	Gaussian
0.8 - 1.5	106 - 144	106 - 144	106 - 148	106 - 148
1.5 - 5	106 - 144	106 - 142	106 - 148	106 - 148
5 - 7	106 - 144	106 - 138	106 - 148	106 - 148
7 - 9.5	106 - 144	107 - 135	104 - 148	106 - 148
9.5 - 30	106 - 144	108 - 133	104 - 148	104 - 148

Table 1: *The energy dependent ToF fit ranges of the different models.*

was introduced. The exponential model and the gaussian model can follow the shape of the ToF contiuum over a considerably wider ToF range (see Fig. 2 in `COM-RP-MPE-DRG-165`). As will be discussed in more detail later in this report, the models can follow the shape of the ToF_{III} distribution even at the highest energies, which was not the case for ToF_{II} data. The energy dependent fit ranges of the different models are summarized in Table 1.

3 Results

3.1 Best Fit Parameter Values

The best fit parameter values for the forward peak obtained from the study of the `GAMMA-1` data ToF_{III} distribution in the forward peak region as a function of Etot are depicted in Fig. 1. For comparison, the result of the analysis of the ToF_{II} distribution (Fig. 4 in `COM-RP-MPE-DRG-165`) is also shown in Fig. 2. The general differences of the three models are the same for ToF_{III} and ToF_{II} data, as are the physics that are reflected in systematic trends. All this has already been discussed in `COM-RP-MPE-DRG-165` and will not be repeated here.

The position of the forward peak ("Centre") still varies with energy, but the amplitude of this variation is smaller for ToF_{III} data than for ToF_{II} data. In addition, the differences in the forward peak position in the three models decreased. At energies below 2.2 MeV the ToF_{III} forward peak position is systematically at lower ToF values than the ToF_{II} forward peak position.

The width of the forward peak decreased at all energies and for all models. Below 9 MeV the forward peak width decreased by about 0.5 channels and at higher energies by almost 1 channel, in very good ageement to the values given in `COM-RP-ROL-DRG-62` by Rob van Dijk for the four standard energy ranges. In addition, the differences between the three models decreased also, and the variation of the forward peak width with energy is smoother for ToF_{III} data than for ToF_{II} data (strong instrumental lines have a smaller impact on the width, as can be seen in the 2.2 MeV line region). Therefore an average forward peak width ("fit") can be defined, which is simply the average of the widths obtained with the three models, fitted in three energy ranges: 0.8 - 7 MeV, 7 - 8.5 MeV and 8.5 - 30 MeV.

The variation of the forward peak position and width with energy is very similar for ToF_{III} and ToF_{II} data. Obviously, the instrumental background changes dramatically between 7 MeV and 9 MeV, as was already pointed out in `COM-RP-MPE-DRG-165`. This change is not an artefact of the ToF correction, but reflects an abrupt change of the physical processes that dominate the instrumental background at a given energy.

The amplitude of the forward peak ("Height") is significantly higher for ToF_{III} data (OPs from Phases 2, 3, 4 and 5) than for ToF_{II} data (OPs from Phases 1, 2 and 3) at all energies. In addition, the intensity of the "1.4 MeV line" feature almost doubled. These differences will be addressed in more detail in Sec. 3.3.

As will be discussed in the following, the three models can fit the distribution of ToF_{III} data *at all energies*, which is not true for ToF_{II} data. This is mostly due to the decrease in the forward peak width.

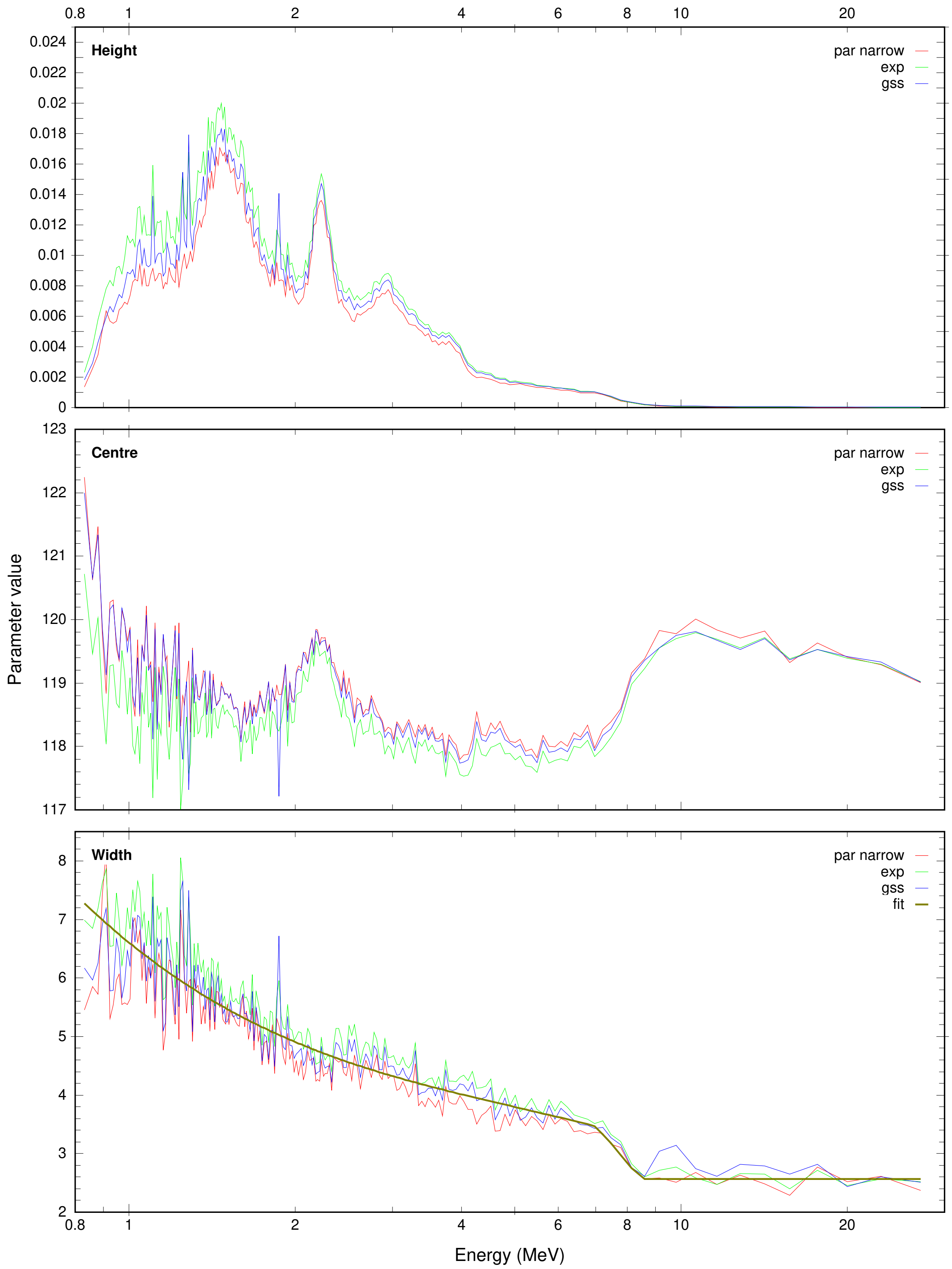

Figure 1: *The best fit values of the parameters describing the forward peak for the parabolic model (narrow range), the exponential model and the gaussian model. "Height" corresponds to the parameter p_1 for all three models. Similarly, "Center" and "Width" correspond to the model parameters p_2 and p_3, respectively.*

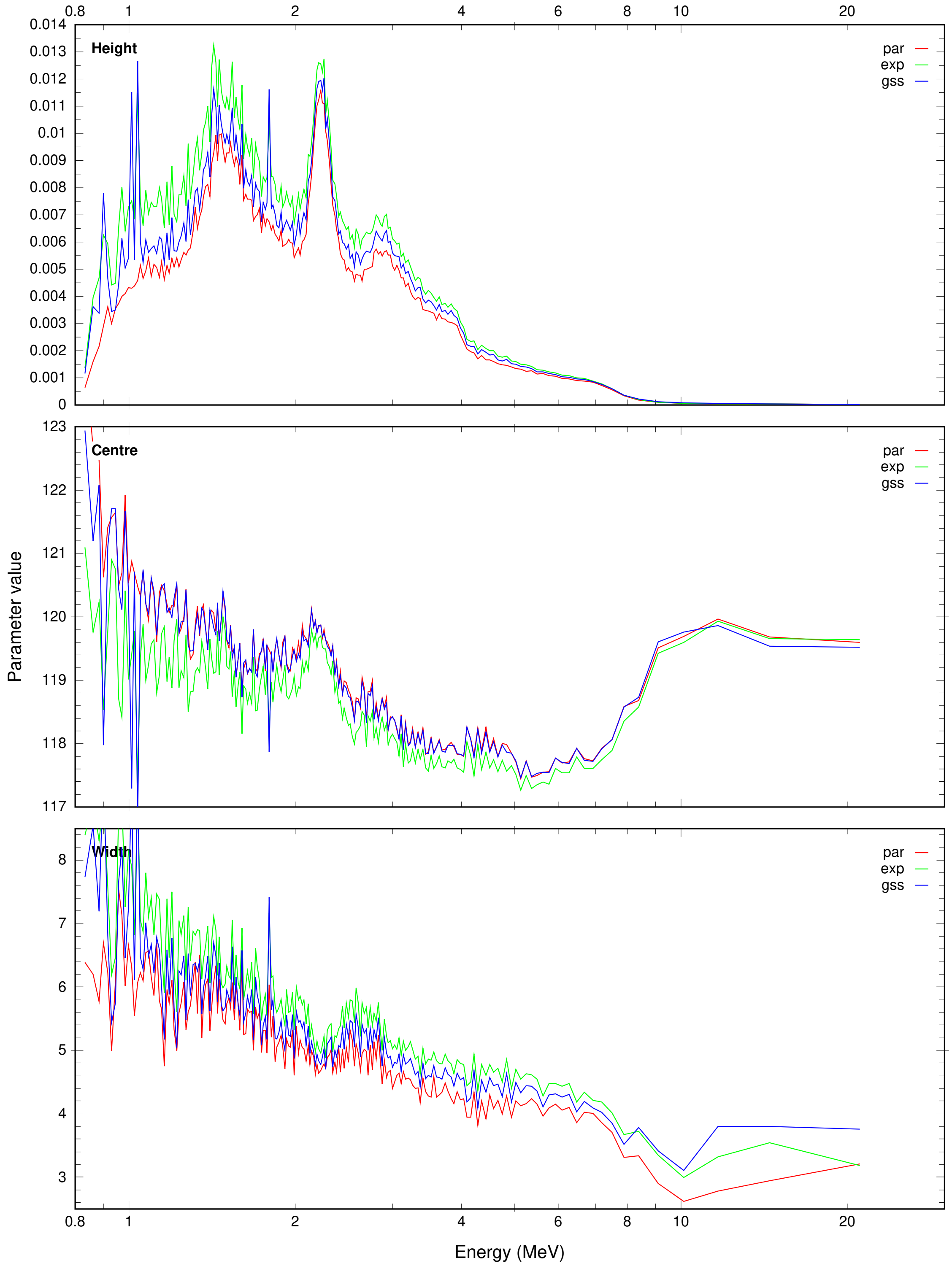

Figure 2: *The best fit values of the parameters describing the "old" ToF$_{\rm II}$ forward peak (this is Fig. 4 from* `COM-RP-MPE-DRG-165`*).*

3.2 Statistical Significance of the Fits

A comparison of the values of χ^2_ν for fits of $\mathrm{ToF_{III}}$ data (top) and $\mathrm{ToF_{III}}$ data (middle and bottom) is shown in Fig. 3. As was pointed out in `COM-RP-MPE-DRG-165`, all three models fail to describe the shape of the $\mathrm{ToF_{II}}$ distribution above about 10 MeV (top). The three models can, however, fit the $\mathrm{ToF_{III}}$ distribution *at all energies* (middle). If the parabolic model is fitted in the narrow range defined in Sec. 2.2.3, then all three models fit the data about equally well. If the wide fit range is used for the parabolic model, then it is clearly worse than the other two models in the energy region from about 10 - 18 MeV. It has to be mentioned, however, that fitting the parabolic model in a narrow range is "forcing" a decrease in χ^2_ν. The parabolic model still does not follow the shape of the ToF distribution at high energies; the narrow range simply cuts off those regions where the discrepancy is sufficiently large to increase χ^2_ν. The values of χ^2_ν obtained in fits of the $\mathrm{ToF_{III}}$ distribution with the width of the forward peak fixed at the average width defined in Sec. 3.1 in all three models are shown at the bottom. Fixing the forward peak position, which reduces the number of free fit parameters from 6 to 5, does *not* change the values of χ^2_ν.

The three models can only fit $\mathrm{ToF_{III}}$ data, but not $\mathrm{ToF_{II}}$ data, above about 10 MeV. Below this energy, however, the values of χ^2_ν seem to indicate that the models follow the $\mathrm{ToF_{II}}$ distribution better than the $\mathrm{ToF_{III}}$ distribution. In particular, the values of χ^2_ν for $\mathrm{ToF_{II}}$ fits show less scatter around an average value of 1. The average χ^2_ν value for $\mathrm{ToF_{III}}$ fits is slightly above 1. In addition, there is a slow but steady increase of the value of χ^2_ν for $\mathrm{ToF_{III}}$ data, but not for $\mathrm{ToF_{II}}$ data. Some of these differences could be due to the different sets of data used for the $\mathrm{ToF_{II}}$ and $\mathrm{ToF_{III}}$ distributions, and to the different statistics.

The $\mathrm{ToF_{II}}$ data base consists of about 8.6×10^6 events with 316431 superpackets from 36 OPs from Phases 1, 2, and 3. Upon the creation of the $\mathrm{ToF_{II}}$ data base no ToF selection was applied. If the same ToF selections had been applied as for the $\mathrm{ToF_{III}}$ database (see Sec. 2.1), then the $\mathrm{ToF_{II}}$ data base would have contained less than 8×10^6 events (the different PSD selections for the two data bases have a minor effect on the number of events). Thus the $\mathrm{ToF_{III}}$ spectra contain on average about 20% more events than the $\mathrm{ToF_{II}}$ spectra, which may explain part of the increase in the average value of χ^2_ν. In addition, the relative contribution of instrumental lines and continuum background to the $\mathrm{ToF_{III}}$ data base is much larger than in the $\mathrm{ToF_{II}}$ data base, as will be discussed in the following. If the various background components are produced in different parts of the telescope or spacecraft they will have different ToF spectra (which in addition depends on the physical process). The superposition of various background components complicates the shape of the ToF spectrum and may also contribute to the increase of χ^2_ν.

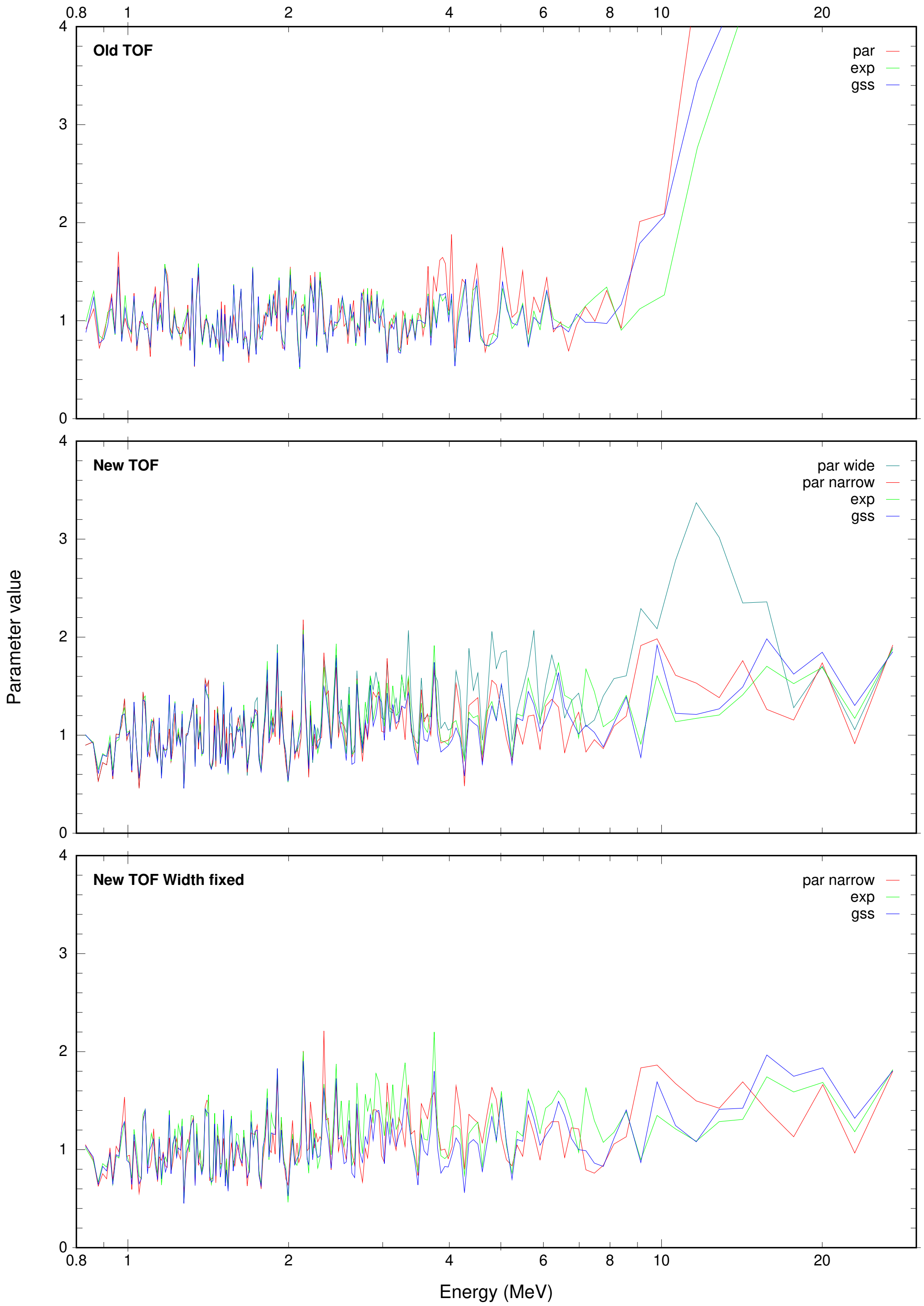

Figure 3: *A comparison of the values of* χ^2_ν *for fits of* ToF_{II} *data (top) and* ToF_{III} *data (middle and bottom).*

3.3 Forward Peak Energy Spectrum

Using the best fit parameter values (the forward peak parametes are depicted in Fig. 1) the energy spectra of the forward peak and of the ToF continuum background were calculated for the ToF range from channel 107 to channel 130. The forward peak spectra for the parabolic model (narrow and wide range), the exponential model and the gaussian model, are depicted in Fig. 4. For each model (except the "wide" parabolic model) the fit with a free forward peak width is compared to the fit with the forward peak width fixed at the average value. Obviously, the fits are stabilized by fixing the width of the forward peak. Below 8 MeV the wide and narrow parabolic models yield practically the same forward peak spectrum. Fixing the forward peak width results in a slight but systematic increase of the parabolic intensity. The exponential intensity slightly decreases, and the gaussian intensity remains the same. This was to be expected from Fig. 1. The forward peak width of the gaussian model is almost identical to the average width, whereas the parabolic and the exponential models yield smaller and higher values, respectively.

In Figs. 5 and 6 a comparison of the forward peak intensity derived from $\mathrm{ToF_{II}}$ data (top, which is identical with the top of Fig. 7 in `COM-RP-MPE-DRG-165`) and from $\mathrm{ToF_{III}}$ data is given for Etot below and above 8 MeV, respectively. In any case, the parabolic models systematically yield the lowest and the exponential models systematically yield the highest forward peak intensities. As was pointed out in `COM-RP-MPE-DRG-165`, for $\mathrm{ToF_{II}}$ data the forward peak intensity for the exponential model is at least 25% larger than for the parabolic model at 1 MeV. At 2.2 MeV the difference still is at least 15% and then slowly decreases with increasing energy. The same is true for $\mathrm{ToF_{III}}$ data, despite the fact that the width of the forward peak decreased. This indicates that the different forward peak intensities for the different models are artefacts from the models. Improving the statistics of the ToF spectra would not reduce the systematic differences of the models. *Since we still cannot tell which of the models (or which other model) best describes the shape of the ToF spectrum, we have to add this systematic difference or uncertainty as a systematic error to all COMPTEL flux measurements based on fits of the ToF forward peak.*

It is obvious from Fig. 5 that the energy spectrum of the forward peak changed significantly after the reboost[2]. In particular, the forward peak event rate in the 1.4 MeV feature (which consists of contributions from ^{40}K, ^{22}Na, ^{24}Na and presumably other instrumental lines) increased dramatically, whereas the changes are small above 2 MeV. It has to be pointed out, however, that the event selections applied in the two sets of ToF analyses are slightly different.

To allow a more quantitative comparison the $\mathrm{ToF_{III}}$ analysis was therefore repeated with the $\mathrm{ToF_{II}}$ event selections and $\mathrm{ToF_{II}}$ energy binning for the gaussian model (which returns an "average" event rate) with the forward peak width fixed at the average value defined in Sec. 3.1 (see Fig. 1). A comparison of the "average Phase 1, 2 and 3" forward peak event rate (derived from $\mathrm{ToF_{II}}$ data) and "average Phase 2, 3, 4 and 5" forward peak event rate (derived from $\mathrm{ToF_{III}}$ data) between 0.8 MeV and 8 MeV is given in Fig. 7. At higher

[2]The $\mathrm{ToF_{II}}$ data base consists of OPs from Phases 1, 2 and 3; the $\mathrm{ToF_{III}}$ data base consists of of OPs from Phases 2, 3, 4 and 5.

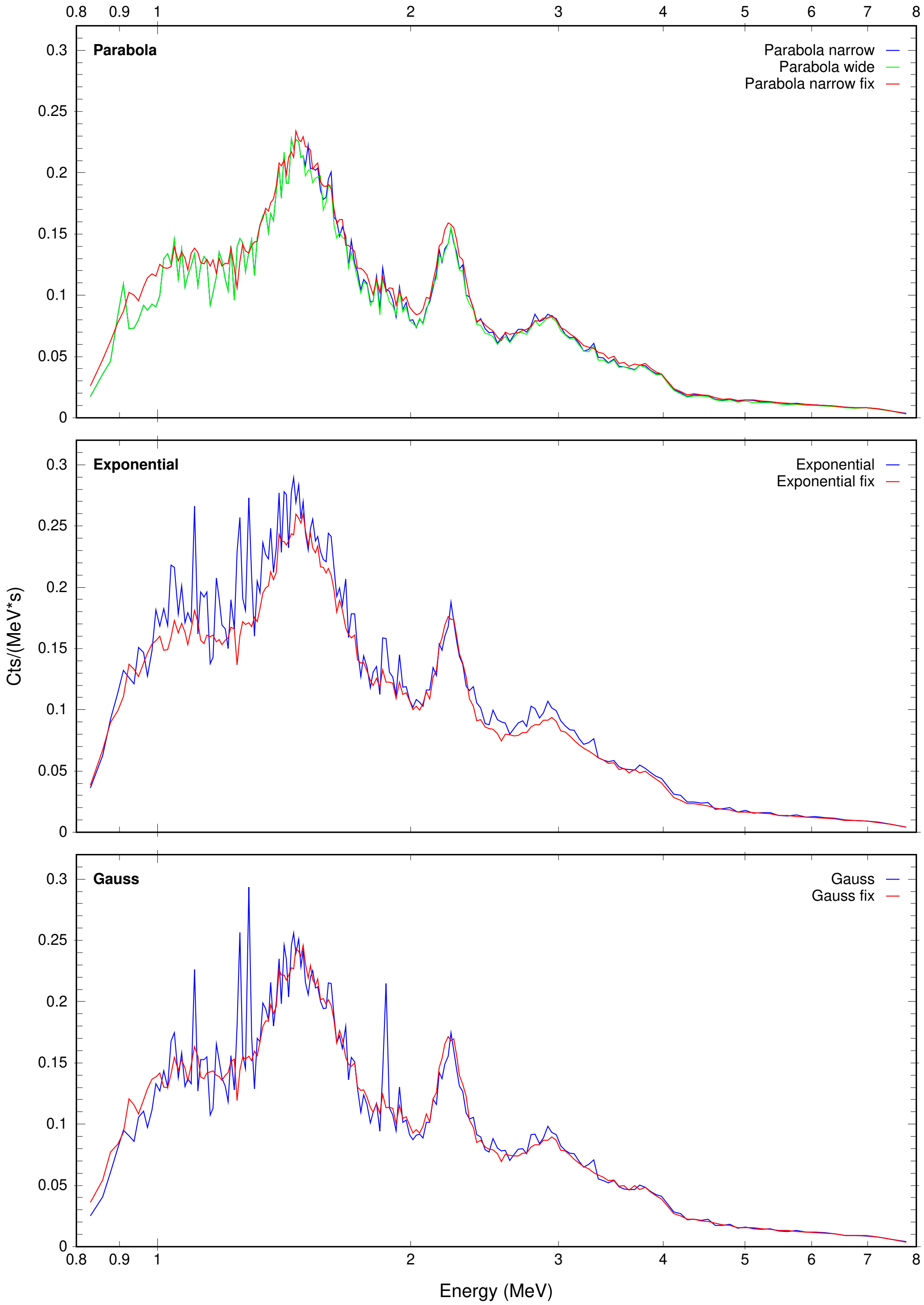

Figure 4: A comparison of the ToF_{III} forward peak intensity from 0.8 MeV to 8 MeV derived with the parabolic model (top), the exponential model (middle) and the gaussian model (bottom).

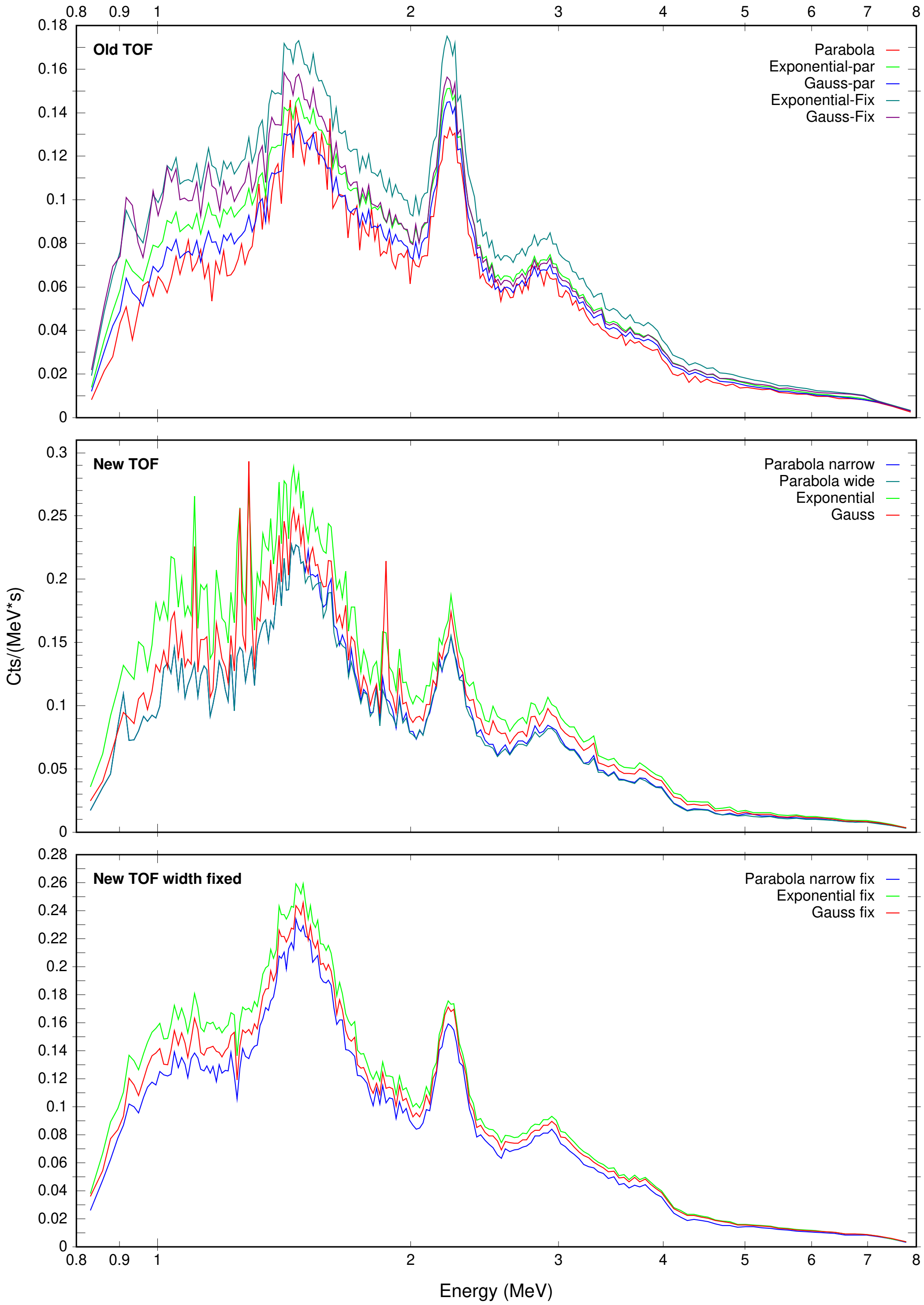

Figure 5: *A comparison of the forward peak intensity from 0.8 MeV to 8 MeV derived from* ToF_{II} *data (top) and* ToF_{III} *data (middle and bottom).*

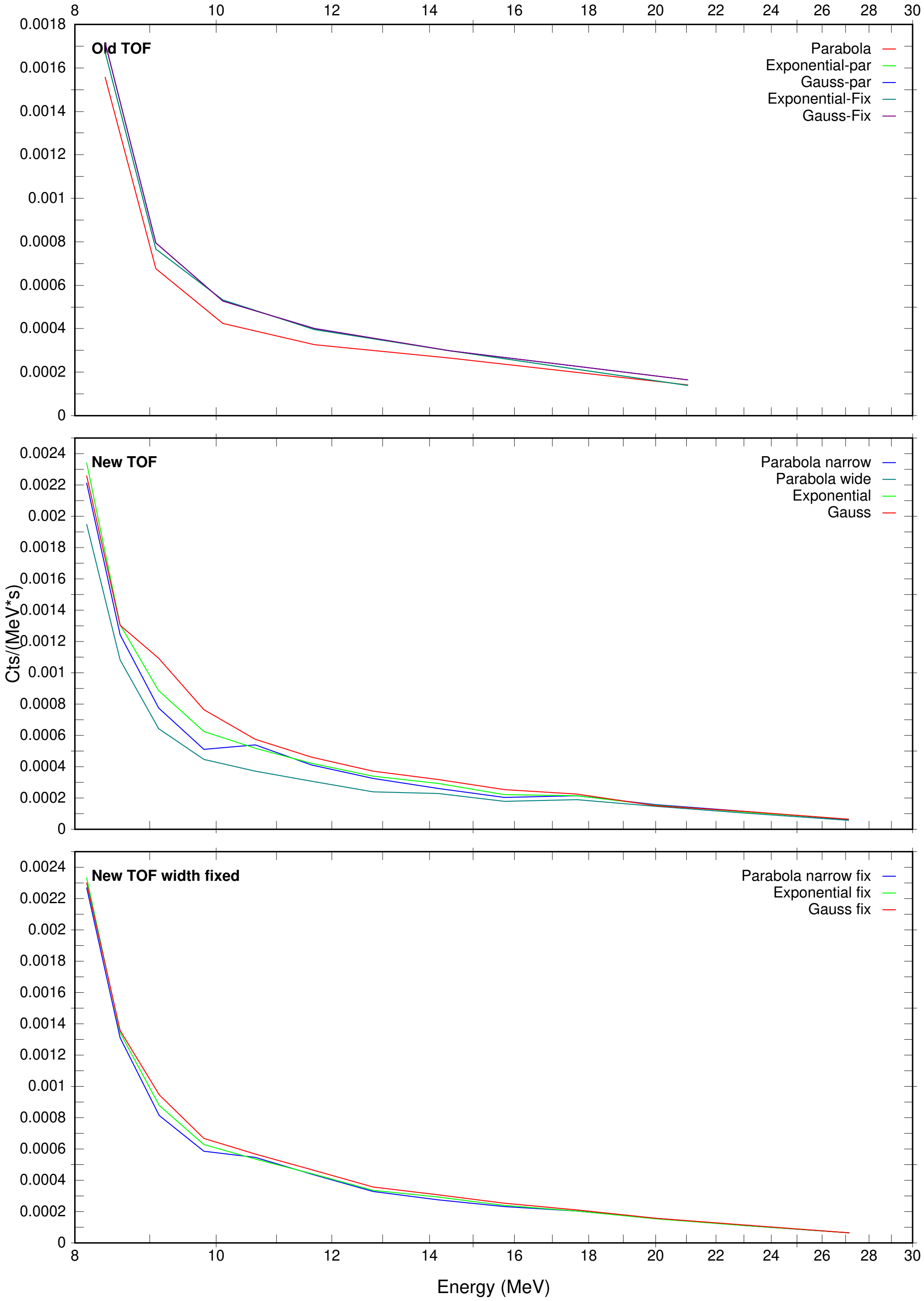

Figure 6: *A comparison of the forward peak intensity from 0.8 MeV to 8 MeV derived from* ToF_{II} *data (top) and* ToF_{III} *data (middle and bottom).*

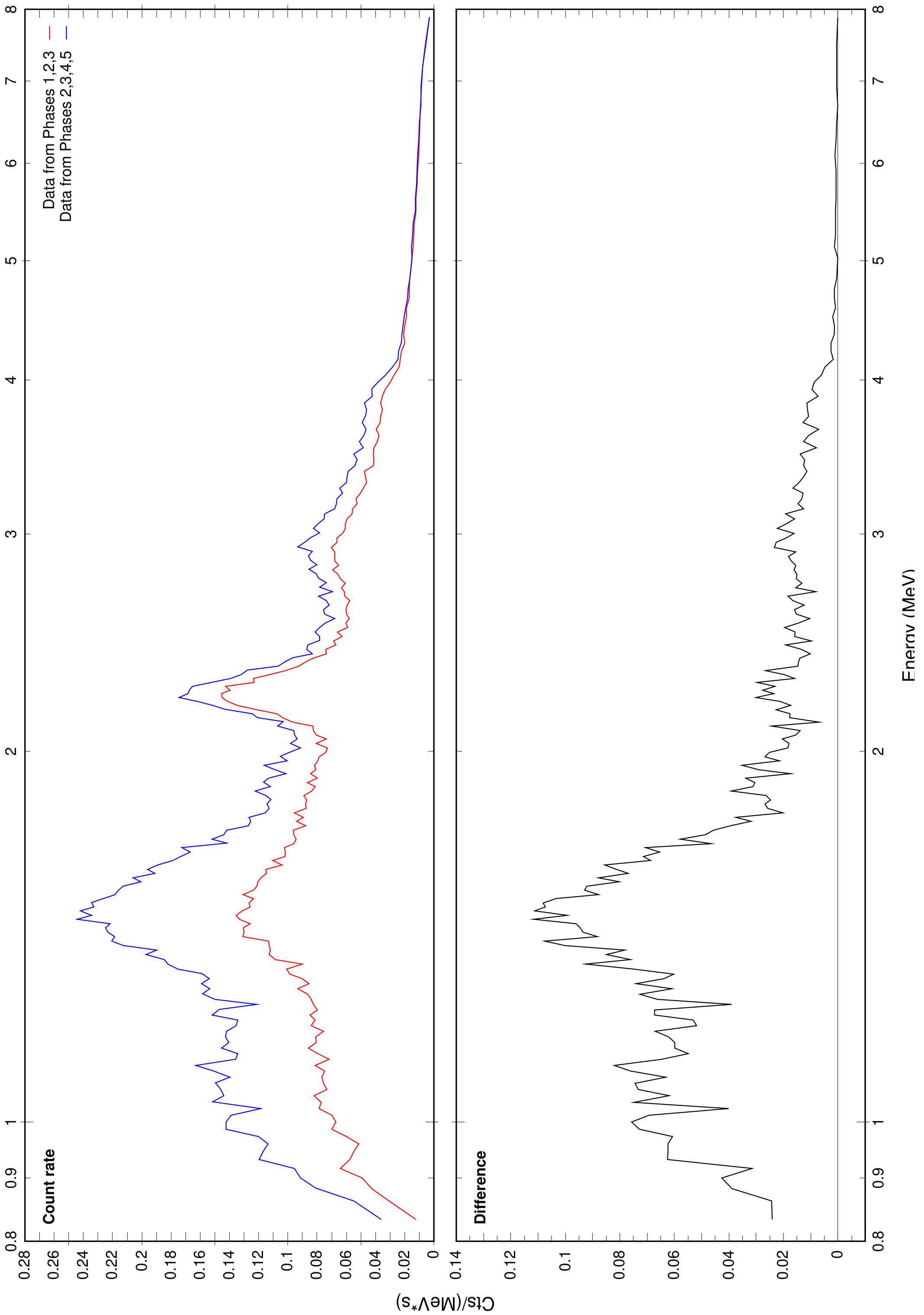

Figure 7: *A comparison of the forward peak intensity from 0.8 MeV to 8 MeV derived from* ToF_{II} *data (which consists of OPs from Phases 1, 2 and 3) and* ToF_{III} *data (which consists of OPs from Phases 2, 3, 4 and 5).*

energies such a comparison is not possible because of the uncertainties of the $\mathrm{ToF}_{\mathrm{II}}$ fits. If the $\mathrm{ToF}_{\mathrm{II}}$ results are taken at face value, then they scatter around the $\mathrm{ToF}_{\mathrm{III}}$ results without deviating more than about 10%. This may indicate that the forward peak event rate above about 4.5 MeV is not significantly affected by cosmic-ray induced activation with life-times between tens of minutes and a few years - in remarkable contrast to the event rates below 4.5 MeV. At these low energies the forward peak spectrum changed dramatically, both the underlying continuum and the instrumental lines on top. The two "humps" above about 2.7 MeV indicate a moderate increase due to the ^{24}Na cascade. It also seems that the 2.2 MeV line from thermal neutron capture on hydrogen slightly increased due to the increased atmospheric neutron albedo during solar minimum. The small excess around 1.9 MeV may be partially caused by the decay of ^{28}Al. The most dramatic changes, however, occur below 1.8 MeV. The upper slope of the huge excess around 1.4 MeV is consistent with the signature of ^{22}Na (see `COM-RP-MPE-SIM-4` by G. Weidenspointner), but other isotopes such as ^{24}Na are also known to contribute in that region. Below 1.2 MeV the scatter of the data does not allow the signature of ^{27}Mg to be identified, although it must be present (see `COM-RP-MPE-DRG-166` by U. Oberlack, M. Varendorff and G. Weidenspointner). A fraction of the "continuum" can already be attributed to the isotopes mentioned above. It remains to be seen whether all of the continuum can be attributed to instrumental lines as they are identified.

3.4 Forward Peak Range

A comparison of the forward peak range, defined as the forward peak position plus or minus the forward peak width, for $\mathrm{ToF_{II}}$ data (top) and $\mathrm{ToF_{III}}$ data (middle and bottom) is depicted in Fig. 8. To fascilitate this comparison, the $\mathrm{ToF_{III}}$ data forward peak range for the parabolic model in the narrow fit range and with fixed forward peak width is included in the $\mathrm{ToF_{II}}$ data plot at the top. As can be seen from this plot, the forward peak range for $\mathrm{ToF_{III}}$ data is systematically shifted to lower ToF values for energies below 2.2 MeV. Therefore the forward peak range varies less with energy. A decrease of the width of the forward peak region is hardly noticable at these low energies. Above 2.2 MeV the situation is different. The center of the forward peak region is about the same for $\mathrm{ToF_{II}}$ and $\mathrm{ToF_{III}}$ data, but the width of the forward peak region is smaller for $\mathrm{ToF_{III}}$ data than for $\mathrm{ToF_{II}}$ data. It is interesting to note that the dramatic change of the shape of the ToF distribution between 8 MeV and 10 MeV is reflected in the forward peak range. As was to be expected from the ToF distribution, the lower boundary of the forward peak region is affected more strongly than the upper boundary.

The three models yield more similar forward peak ranges for $\mathrm{ToF_{III}}$ data (middle) than for $\mathrm{ToF_{II}}$ data (top). If the width of the forward peak is fixed in the $\mathrm{ToF_{III}}$ fits at the average value defined in Sec. 3.1 (see Fig. 1), then the forward peak range is almost independent of the model used (bottom). This means that the position of the forward peak then is almost independent of the model used. The "true" width and position of the forward peak are only determined by the physics of the instrument (and the event selections). The fact that all three models yield practically the same forward peak position/range if the width of the forward peak is fixed shows that the definition of the average forward peak width closely reflects the physics of the instrument (and the particular set of event selections).

Acknowledgement:

This study would not have been possible without the kind support and the "encouragement" of the Gummibärchen-Connection, Uncle Tom and the Smouldering Dragon, respectively.

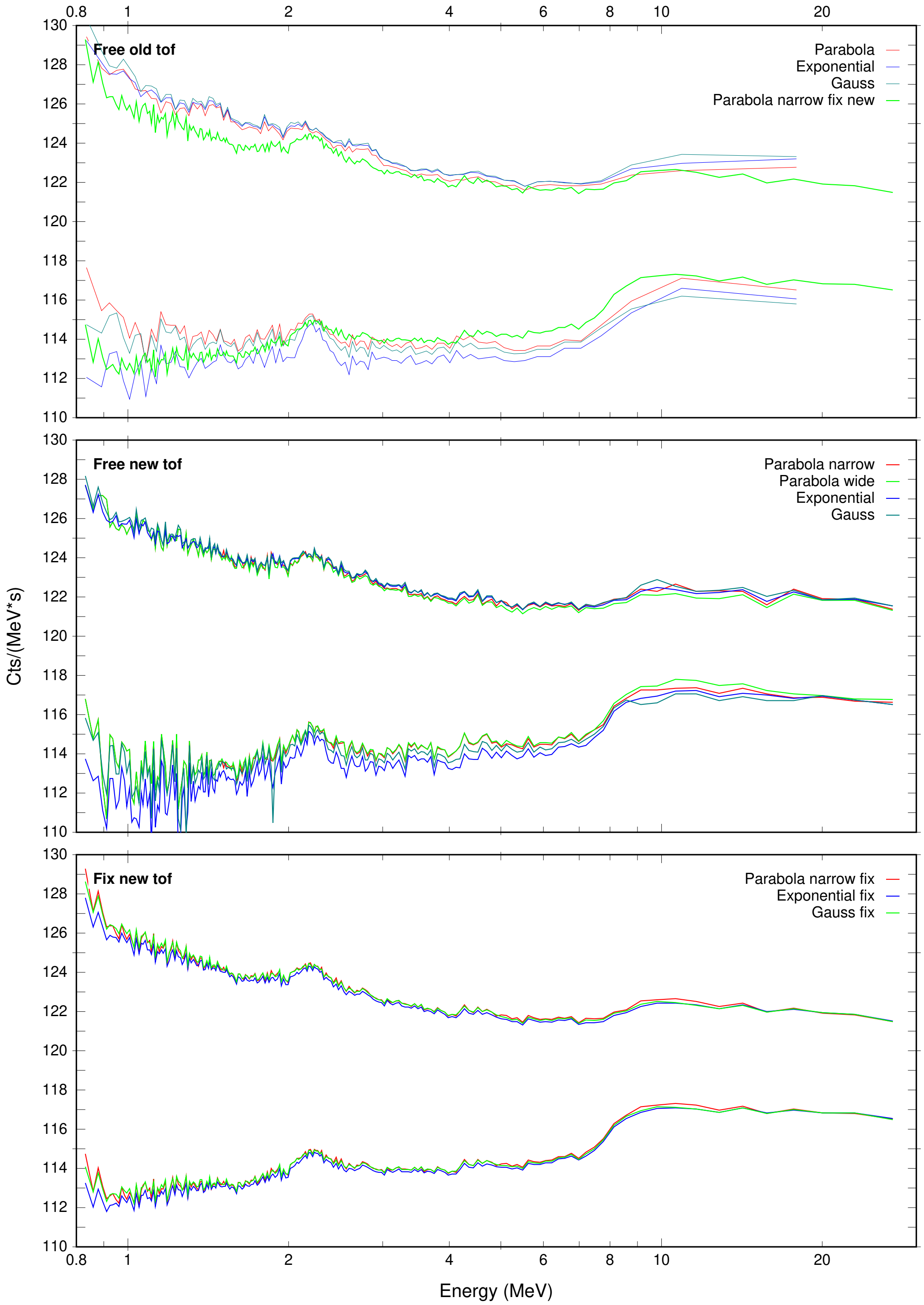

Figure 8: A comparison of the forward peak range derived from ToF_{II} data (top) and ToF_{III} data (middle and bottom).